Journal of the European Ceramic Society 15 (1995) 1235–1247
Elsevier Science Limited
Printed in Great Britain.
0955-2219/95/$9.50
0955-2219(95)00098-2

The Complexity of the Matrix Microstructure in SiC-Fiber-reinforced Glass Ceramic Composites

Franck Doreau, Hélène Maupas, Dominique Kervadec, Pierre Ruterana, Jean Vicens & Jean-Louis Chermant

LERMAT, URA CNRS n°. 1317, ISMRA, 6 Bd du Maréchal Juin, 14050 Caen Cedex, France

(Received 1 December 1994; accepted 25 May 1995)

Abstract

In this paper a critical examination of the diagrams of different silicate systems is presented: LAS, MAS YAS, MLAS and YMAS (A: alumina; L: lithia; M: magnesia; S: silica; Y: yttria). These systems have been developed to fabricate ceramic matrix composites based on a glass ceramic matrix, because of their low thermal expansion coefficient and good mechanical properties up to 1000°C. The observations and microanalyses, by transmission electron microscopy, of different batches of MLAS and YMAS confirm the complexity of the systems investigated.

Introduction

The new class of materials known as ceramic matrix composites (CMCs) is concerned with a ceramic matrix reinforced either by ceramic fibers, whiskers or particles. But the matrix could be (i) a monolithic ceramic — such as SiC, Al_2O_3, Si_3N_4... — or (ii) a glass ceramic. The first ones are prepared for CMC materials from the ceramic routes, that is to say sintering or chemical vapour infiltration (CVI) processes, and the second ones result from the glass route which is easier and needs a lower process temperature. Nevertheless the domain of applications of glass ceramic matrices is lower than for ceramic matrices — the 1000°C domain —, but is of interest for specific applications in parts for motor aerospace and aircraft engines due to their strength and low densities (~2·5).

The scope of this paper is to present and to comment upon the complexity of several glass ceramic matrices which occur due to the crystallographic characteristics of many silicate phases which can arise in a very narrow domain of temperatures and, moreover, which can also lead to allotropic transformations and/or ionic substitutions in the same temperature domain.

Due to the fact that the lithium aluminum silicate (LAS) system has crystalline phases with a very low thermal expansion coefficient, and because these phases can appear in a very controlled way, this system is one that is investigated most to fabricate CMCs. But we shall see that such a system is in fact extremely complex. To fabricate CMCs with SiC Nicalon fibers and a glass ceramic matrix, several requirements are necessary: the glass ceramic must be chemically compatible with the SiC fibers (or alumina fibers) in order to avoid a resultant fibers degradation. Moreover the matrix and fibers must have an elastic modulus different enough and a thermal expansion coefficient low enough to have a reinforced material which is not damaged during the process. Finally such materials have to involve a correct pull-out process to exhibit a good mechanical strength. The LAS system is the most suitable but there are other systems which also seem promising, but with some advantages and disadvantages:[1] CAS, MAS, YAS,... for ternary systems, or BMAS, MLAS, YMAS,... for quartenary systems. Among these different systems, we shall discuss the LAS, MAS, YAS, MLAS and YMAS systems.

The LAS, MAS and MLAS Systems

The Li_2O–Al_2O_3–SiO_2 system gives a wide range of compositions with the thermal expansion coefficient ranging from 0 to about 120 $10^{-7}°C^{-1}$.[2] These materials have a very good thermal shock resistance and consequently they are used either for cooker panels, saucepans, or for specific optical devices for space applications such as blanks for laser gyroscopes or for X-ray telescopes.[3] But this thermal expansion coefficient is considerably affected by the existence of some crystalline phases: for example, if the alumina content is low, the materials present a higher thermal expansion coefficient, while if its content is high, the result is a material with a zero thermal expansion value.

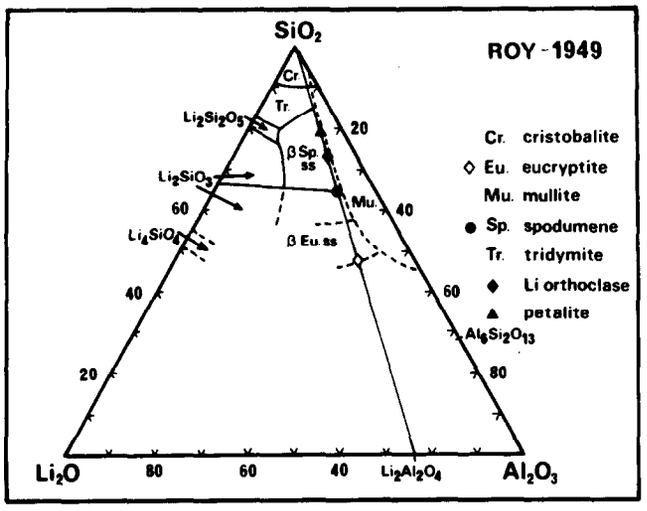

Fig. 1. Ternary diagram of phase equilibria of the Li_2O–Al_2O_3–SiO_2 system (LAS)[4]

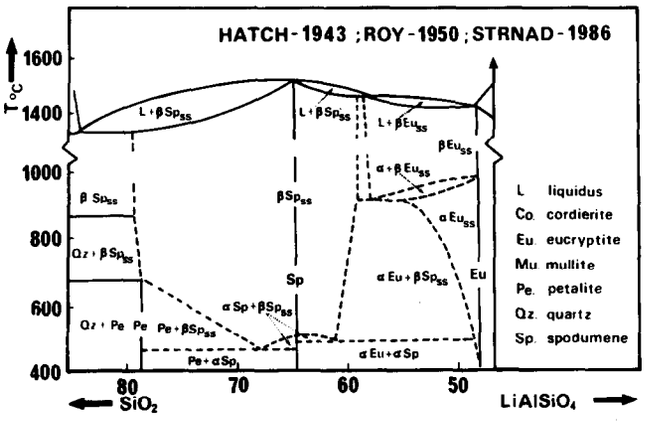

Fig. 2. Pseudo binary diagram of phase equilibria of the eucryptite–silica (Li_2O–Al_2O_3–$2SiO_2$–SiO_2) system.[4,5,7]

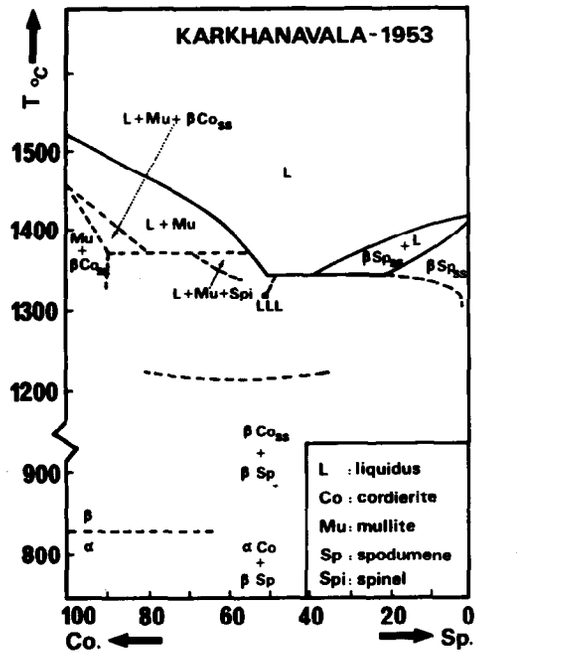

Fig. 3. Pseudo binary diagram of phase equilibria of the cordierite–spodumene (Co–Sp) ($2MgO$–$2Al_2O_3$–$5SiO_2$–Li_2O–Al_2O_3–$4SiO_2$) system (LLL: low limit of liquidus) after using the new nomenclature for α and β cordierite.[8]

There are no recent phase diagrams concerning the Li_2O–Al_2O_3–SiO_2 ternary system. The diagram proposed by Roy and Osborn in 1949[4] and by Roy *et al.* in 1950[5] is still used (Fig. 1). In this diagram we can see the presence of many different silicate phases such as β eucryptite, lithium orthoclase, mullite, petalite, β spodumene and tridymite.

Also useful are the pseudo binary diagrams eucryptite–silica which has also been reported by Hatch,[6] Roy *et. al.*[5] and slightly modified by Strnad in 1986 [7] (Fig. 2), and the pseudo binary diagram, cordierite–spodumene, proposed by Karkhanavala and Hummel,[8] (Fig. 3). For the latter diagram, we have used the new nomenclature for α cordierite (pseudo-hexagonal orthorhombic or low cordierite) and β cordierite (hexagonal or high cordierite).[9] Table 1 shows the crystallographic characteristics of some silicate phases which could appear in different M–M'–Si–O systems.[10]

From these three diagrams, the information from the works of Roy *et. al.*[4,5] and Karkhanavala and Hummel[8] concerning the eucryptite, spodumene, petalite and cordierite phases, and the eucryptite–silica and cordierite–spodumene pseudo binary systems, one can say:

Eucryptite: Li_2O–Al_2O_3–$2SiO_2$

— α eucryptite inverts into the high temperature form, β eucryptite, at 972 ±10°C during an incongruent melting;
— α eucryptite is rhombohedric, with the aluminum atoms in 6 coordination;
— it has been shown by Winkler[11] and also by Roy *et. al.*[5] that the structure of the β eucryptite is the same as that of the high temperature quartz, where the aluminum atoms are in the $A10_4$-tetrahedra.

Spodumene: Li_2O–Al_2O_3–$4SiO_2$

— the spodumene corresponds to the one found in the nature and to the high temperature form called β spodumene;
— the α form inverts in the β high temperature form at a maximum temperature of 500°C;
— it is a monoclinic pyroxene, with a tetragonal type structure.

Petalite: Li_2O–Al_2O_3–$8SiO_2$

— petalite is decomposed congruently to a β spodumene solid solution at 680± 10°C.

Cordierite: $2MgO$–$2Al_2O_3$–$5SiO_2$

— cordierite can appear in three crystallographic forms:[9]

(i) two low temperature forms, the stable low temperature α cordierite, which inverts reversibly to the high temperature β form at

Table 1. Crystallographic characteristics of different silicate phases which can appear in M–M'–Si–O systems

Name	*Formula*	*Crystallographic structure*	*Lattice parameters*					
			a Å	*b* Å	*c* Å	α	β	γ
Kyanite	Al_2SiO_5 Al_2O_3,SiO_2	Triclinic	7·112	7·844	5·574	90·09	101·11	105·99
Sillimanite	Al_2SiO_5 Al_2O_3,SiO_2	Orthorhombic	7·49	7·67	5·77	—	—	—
Mullite	$Al_6Si_2O_{13}$ $3Al_2O_3,2SiO_2$	Orthorhombic	7·546	7·690	2·884	—	—	—
Enstatite	$MgSiO_3$ MgO,SiO_2	Orthorhombic	18·23	8·84	5·19—	—	—	—
Protoenstatite	$MgSiO_3$ MgO,SiO_2	Orthorhombic	9·25	8·74	5·32—	—	—	—
Clinoenstatite	$MgSiO_3$ MgO,SiO_2	Triclinic	10·00	8·934	5·17	88 27	70 03	91 09'
Forsterite or Olivine	Mg_2SiO_4 $2MgO,SiO_2$	Orthorhombic	4·756	10·195	5·981	—	—	—
α Yttrium silicate	$Y_2Si_2O_7$ $Y_2O_3,2SiO_2$	Triclinic	6·59	6·64	12·25	94°00	89°20	93°10'
β Yttrium silicate or Keivite	$Y_2Si_2O_7$ $Y_2O_3,2SiO_2$	Monoclinic	6·875	8·970	4·721	—	101°74	—
Spinel	$MgAl_2O_4$ MgO,Al_2O_3	Cubic	8·0831	8·0831	8·0831	—	—	—
α Cordierite	$Mg_2Al_4Si_5O_{18}$ $2MgO,2Al_2O_3,5SiO_2$	Orthorhombic	9·721	17·062	9·339	—	—	—
β Cordierite or Indialite	$Mg_2Al_4Si_5O_{18}$ $2MgO,2Al_2O_3,5SiO_2$	Hexagonal	9·770	—	9·352	—	—	—
Sapphirine	$Mg_2Al_4SiO_{10}$ $2MgO,2Al_2O_3,SiO_2$	Monoclinic	9·94	14·40	9·79	—	110°50	—
α Eucryptite	$LiAlSiO_4$ $Li_2O,Al_2O_3,2SiO_2$	Hexagonal	13·48	—	9·001—	—	—	—
β Eucryptite	$LiAlSiO_4$ $Li_2O,Al_2O_3,2SiO_2$	Monoclinic	5·251	5·259	11·162	—	—	119°83
α Spodumene	$LiAlSi_2O_6$ $Li_2O,Al_2O_3,4SiO_2$	Monoclinic	9·52	8·32	5·25	—	111°20	—
β Spodumene	$LiAlSi_2O_6$ $Li_2O,Al_2O_3,4SiO_2$	Tetragonal	7·538	—	9·156	—	—	—
Lithium orthoclase	$LiAlSi_3O_8$ $Li_2O,Al_2O_3,6SiO_2$	Orthorhombic	18·24	10·54	10·57	—	—	—
Petalite	$LiAlSi_4O_{10}$ $Li_2O,Al_2O_3,8SiO_2$	Monoclinic	15·18	5·139	11·75	—	112°38	—
Lithium magnesium silicate	Li_2MgSiO_4 Li_2O,MgO,SiO_2	Orthorhombic	6·32	10·66	4·99	—	—	—

830°C under hydrothermal conditions, and the metastable μ cordierite which is produced by the glass crystallization in air at about 850°C;

(ii) one high temperature form which can be produced by heating the material or by crystallizing the glass at temperatures between 1000 and 1400°C; at 1460°C the material is decomposed into mullite and liquid, with a complete melting at 1530°C.

Eucryptite–silica

— from these diagrams and the authors' comments,[5] there exists the possibility that a complete series of solid solutions occur between β eucryptite and β spodumene at high temperature;

— crystals of α spodumene are formed in the 375–500°C range;

— spodumene is stable only until 500± 15°C;

— petalite is found to invert completely to β spodumene at about 700°C.

Cordierite–spodumene

— the pseudo binary system cordierite–spodumene[8] is also of interest;

— it shows that α cordierite, α cordierite solid solution, β cordierite, β spodumene, β spodumene solid solution (which is partially metastable) are identified phases, but with also the presence of corundum, mullite and spinel;

— the spinel phase could probably be a solid solution of Li and Mg spinels.

The MAS ($MgO–Al_2O_3–SiO_2$) system was originally investigated by several authors, Rankin and Merwin in 1918, modified by Bowen and Greig in 1924 and Greig in 1927 and was reported by Prokopowicz and Hummel in 1956.[12] Some details have been more recently reported by Osborn and Muan,[13] Jouenne[14] and Partridge *et. al.*[2] (Fig. 4). There is little information regarding the MLAS

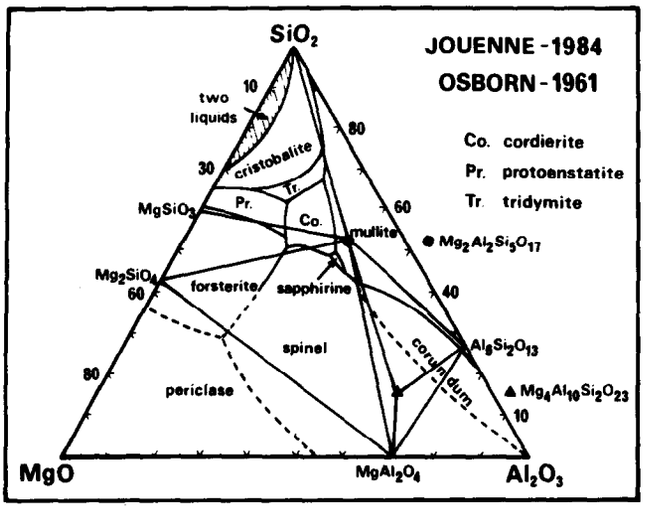

Fig. 4. Ternary diagram of phase equilibria of the $MgO–Al_2O_3–SiO_2$ system (MAS).[13]

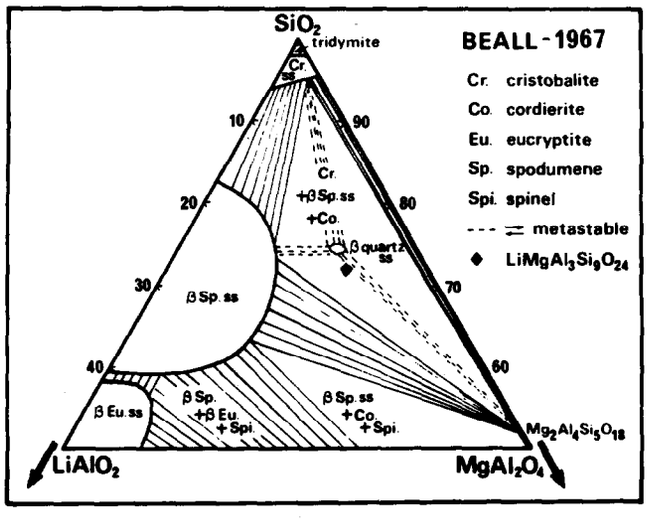

Fig. 5. Isothermal section at 1230°C for the pseudo ternary diagram of the $SiO_2–LiAlO_2–MgAl_2O_4$ system (MLAS).[15]

($MgO–Li_2O–Al_2O_3–SiO_2$) system,[12,15,16] (Fig. 5). It is based on cordierite ($2MgO–2Al_2O_3–5SiO_2$) and protoenstatite (or clinoenstatite (another allotropic form) according to different authors) ($MgO–SiO_2$), with other crystal phases: cristobalite (SiO_2), forsterite ($2MgO–SiO_2$), mullite ($3Al_2O_3–2SiO_2$) and spinel ($MgO–Al_2O_3$), and with the nucleating agents for cordierite based materials: TiO_2 or a combination of $TiO_2–ZrO_2$. As for LAS, it was found by Barry *et. al.*[17] that following the formation of the nucleating phase (a magnesium aluminosilicate structurally similar to the petalite), a number of intermediate phases appears prior to the development of the cordierite at about 1150–1250°C.

At high temperatures the relationships between spodumene and cordierite are very complex and involve also corundum, mullite and spinel, while at low temperatures, there exists a complete series of metastable solid solutions between μ cordierite and β spodumene.

In Ref. 18 details on the preparation of MLAS glass ceramic materials from a glass powder are given either by a traditional route (melting, nucleation and crystallization) or by simultaneous sintering and crystallization. The last method is largely cost-saving as it reduces the time at the fabrication temperature due to the difference in the viscosity. The interest of such a system (MLAS) is the ability to adjust the properties such as the thermal expansion coefficient, softening temperature, viscosity or the dielectric constant according to the chemical composition. Moreover it has been proved that the addition of MgO to $Li_2O–Al_2O_3–SiO_2$ glasses modifies the nonbridging oxygen, and consequently affects the bond strength, with a direct consequence on the glass transition temperature (T_g) of the MLAS.[19]

In the two pseudo ternary systems LAS and MAS, there exists equivalent crystallographic phases where cations can be located in a position of insertion. So it could be possible to combine the low values of the thermal expansion coefficient of LAS with the excellent mechanical properties of MAS. From the pseudo binary diagram,[8] there is effectively a large domain where there are both β spodumene solid solution and β cordierite. Moreover due to the similar sizes of Li^+ (0·68 Å) and Mg^{2+} (0·78 Å) there is a possible substitution which reinforces the glass ceramic phase.[15,20] Recently it has been shown that, in the presence of boron, there is also a substitution of boron for aluminum in the β eucryptite structure.[21]

The YAS and YMAS Systems

Systems based on Y_2O_3 are interesting because of

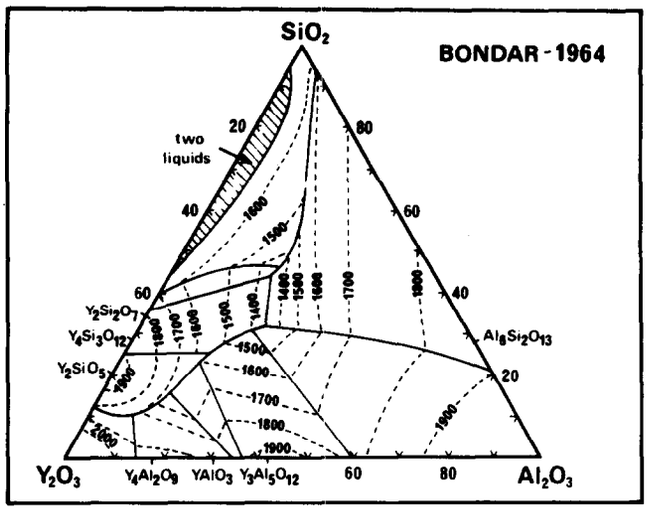

Fig. 6. Isothermal sections for the ternary diagram of the Y_2O_3–Al_2O_3–SiO_2 system (YAS).[24]

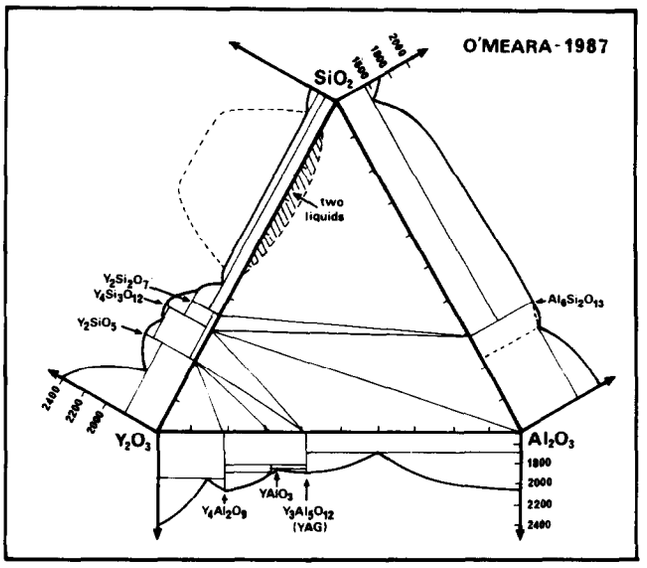

Fig. 7. Ternary and binary diagrams of phase equilibria of the Y_2O_3–Al_2O_3–SiO_2 system (YAS).[22]

its refractory nature and its oxidation resistance. Although the Y_2O_3–Al_2O_3–SiO_2 (YAS) system is extremely important for the understanding of sialons and β Si_3N_4 based ceramics containing Al_2O_3 and Y_2O_3 as sintering additives,[22] there is little information on this phase diagram. One can also note that this system was also investigated to develop YAS glass microspheres for radiotherapeutic applications (the ^{90}Y isotope being activated *in situ* by neutron bombardement, while Al, Si and O are not affected).[23]

Bondar and Galakov proposed a ternary diagram in 1964,[24] (Fig. 6), which was reinvestigated more recently by O'Meara *et al.* in 1987,[22] (Fig. 7). The crystalline identified phases are mainly yttrium disilicate (Y_2O_3–$2SiO_2$) under the two forms α and β (α being the main crystalline product), YAG ($3Y_2O_3$,$5Al_2O_3$) and mullite ($3Al_2O_3$,$2SiO_2$). However, Y_2O_3, Al_2O_3, and some other phases are unidentifiable using classical X-ray tables.

The YAS system has been investigated, more recently.[23] Ten glasses were fabricated at $T<1800$°C, each one corresponding to a specific composition. Among them only one gave a partially crystallized material. These authors were able to give some information and comments on the ternary diagram. As for the LAS system, the thermal expansion coefficient varies significantly with increasing the Y_2O_3 content, while it decreases as SiO_2 is added.[1] One of these compositions was also investigated later by other authors.[1] Their attention was focused on the fact that for the four polymorphic transformations of the $Y_2Si_2O_7$ phase, three different temperatures are reported for each transformation according to three different authors, (Table 2).[25–27] Moreover they found that the triclinic α form inverts in the β monoclinic form at 1285°C. In order to obtain good mechanical behaviour they proposed to sinter these materials above 1300°C to induce β $Y_2Si_2O_7$, otherwise brittle fracture behaviour will occur, which is an undesirable effect for CMC applications[1] as there is a change in the atomic volume associated with the allotropic transformations.[28]

Due to the fact that the distribution of the

Table 2. Yttrium pyrosilicate polymorphic characteristics[1,28]

Transition (volume change)	*Temperature of transition °C*	*Reversibility*	*References*
$\alpha \rightarrow \beta$			
triclinic monoclinic	1190 ± 50	No	Felsche, 1970[26]
(+6·233%)	1225 ± 10	No	Ito & Johnson, 1968[25]
	1225	Yes	Liddell & Thompson, 1986[27]
$\beta \rightarrow \gamma$	1350 ± 30	No	Felsche, 1970[26]
monoclinic monoclinic	1445 ± 10	No	Ito & Johnson, 1968[25]
(–0·198%)	1445	Yes	Liddell & Thompson, 1986[27]
$\gamma \rightarrow \delta$	1580 ± 30	Yes	Felsche, 1970[26]
monoclinic orthorhombic	1535 ± 10	Yes	Ito & Johnson, 1968[25]
(–1·733%)	1535	Yes	Liddell, Thompson, 1986[27]
($\beta \rightarrow \delta$:–1·984%)			

$Y_2Si_2O_7$ particles in these glasses is sufficiently uniform and dilute, Arita *et al.*[29] have recently investigated the nucleation and crystallization of different glass compositions in the system Y_2O_3–Al_2O_3–SiO_2. They found that it is very sensitive to the initial composition of the glass, that Al_2O_3 enhances the sinterability of such a system, and that some specific heat treatment allows us to crystallize all or part of the amorphous phase: that may result in improving their mechanical behaviour and particularly their creep resistance, and will be useful to know for further investigations.

There is no published quaternary diagram on the YMAS system. To our knowledge the only information on the two ternary MAS and YAS systems comes from Refs 30 and 31. Regarding the process and the relationships between the process and crystallographic phases appearing, one can make the following points.

In these materials there are mainly α $Y_2Si_2O_7$, cordierite ($2MgO$–$2Al_2O_3$–$5SiO_2$), and some spinel crystals. Up to 1200°C, the cordierite and α yttrium silicate ratios evolve very slightly, while for a temperature greater than 1230°C, the ratio of α $Y_2Si_2O_7$ decreases significantly while the β $Y_2Si_2O_7$ phase appears; this also corresponds to a decrease in the density (4·30 → 4·03).[25] If there is the presence of yttria, then the low temperature cordierite crystallizes. If the sintering temperature is well chosen (> 1200°C) and the heating rate fast enough to have a short treatment period at $T > 1200$°C to avoid the crystallization of the β $Y_2Si_2O_7$ phase, then the densification is complete within few minutes. So such materials must be fabricated in compromised conditions: at a temperature not too high, but high enough to have a good microstructure and a density not too far from the theorical one. As it has been shown in Ref. 1, in the case of the SiC–YAS composites, the rupture of SiC_f–YMAS also becomes less catastrophic with some pull-out if the temperature process is higher than 1250°C.

Materials and Techniques

Materials investigated in this paper were experimental CMCs with glass ceramic matrices reinforced with Nicalon NLM 202 SiC fibers (Nippon Carbon, Japan). Two types were studied.

SiC_f–MLAS composites were CMCs developed by Aérospatiale (Etablissement de Bordeaux France). The matrix was produced by a chemical sol–gel route. After drying the slurry of a $0{\cdot}5MgO$–$0{\cdot}5Li_2O_3$–$Al_2O_3 4SiO_2$ initial composition which impregnated SiC bundles, tapes are formed, stacked and then densified in a hot press under pressure, in the 1200–1300°C domain.[16,32] Two temperatures were used, T_1) and T_2 ($T_2 > T_1$). The phase crystallization is in fact obtained in controlling the pressing temperature (T_1 or T_2) as well as the cooling rates. The stability of the matrix depends upon the crystalline nature of the matrix phases. In the presence of the β eucryptite solid solution, the stability is limited to 1050°C in the MLAS system (and only to 950°C in the LAS system), (see for example Figs 1 and 5). Above this temperature there is the β eucryptite → β spodumene transformation which modifies the thermomechanical equilibria as the thermal expansion coefficients α are different. Then the new composite possesses new properties (α, σ_r, ...)[32] As-received materials were plates 120 × 100 × 3 mm^3 with either a 1D texture or a $(0–90°)_{ns}$ cross–ply texture, with n = 2 or 3 and *s* meaning for symmetry (Fig. 8(a)).

SiC_r–YMAS composites were fabricated by ONERA (Etablissement de Palaiseau, France) either by a chemical route from organometallic salts and a colloidal sol, or by a glassy route from oxide melting. The initial chemical compositions were always a mixture of oxides: Y_2O_3–MgO–Al_2O_3–SiO_2. Two composites were particularly investigated: Composite A for which the binder burnout is realized in a specific furnace at 700°C under air, while for Composite B it occurs during the hot pressing cycle at 500°C under vacuum.

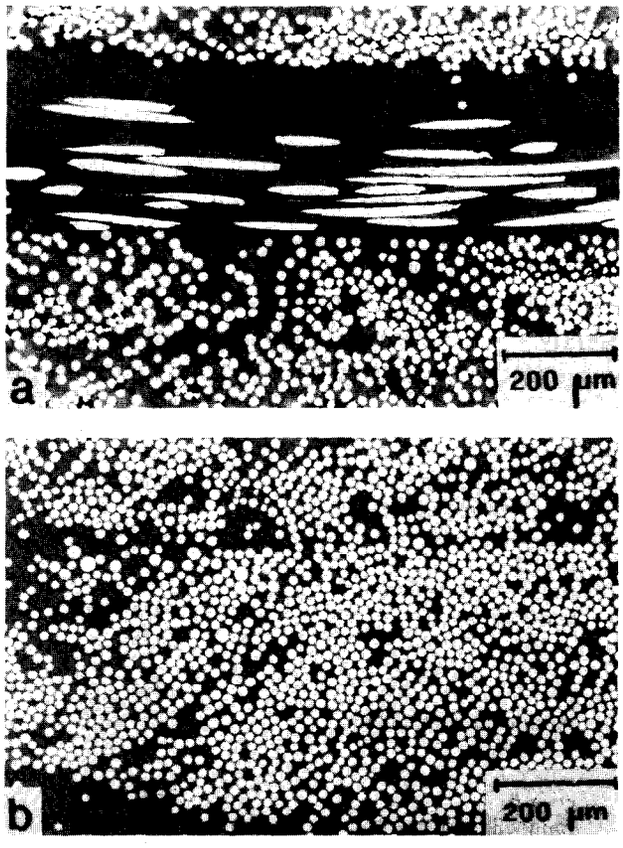

Fig. 8. Optical micrographs of the 2D SiC_f–MLAS (a) and of the 1D SiC_f–YLAS (b) composites.

Composite A is pressed under 10 MPa from 1000°C until 1300°C for 1 hr and then ceramised at 1200°C. Composite B, preloaded under 2 MPa from 500°C, is heated under vacuum until 500°C and pressed under 10 MPa when the maximum temperature, is reached (about 1300°C), and then ceramised at about 1200°C as for Composite A, the vacuum being maintained only until 700°C. Composites A are densified to 98% of the theoretical density and composites B up to the theoretical density. As-received materials were plates 100 × 100 × 3·5 mm^3 with a 1D texture (Fig. 8(b)).

All the specimens were cut with great care and very slowly using diamond wheels: either plates for rupture and creep experiments, or small samples inserted into cylinders of 3 or 2·7 mm in diameter and then cut. These last specimens were mechanically ground up to 50–100 μm, a dimpler was used to thin them up to about 10 μm and finally ion milled under argon (6 kV) at liquid nitrogen temperature (Gatan Duo Mill, Pleasanton, USA).

Microstructural investigations were performed: (i) by X-ray analysis; (ii) by transmission electron microscopy with a Jeol 200 CX and with a Topcon EM 002B: these two TEM operating at 200 kV, were equipped with a Kevex EDS microanalyser and were used to perform TEM, HREM and microanalysis studies; (iii) by scanning electron microsocopy with a Jeol 840 GLS with a Tracor 5200 EDS system, and a Zeiss DSM 60 with a Kevex system and (iv) by an electronprobe analyzer Jeol 6300 F.

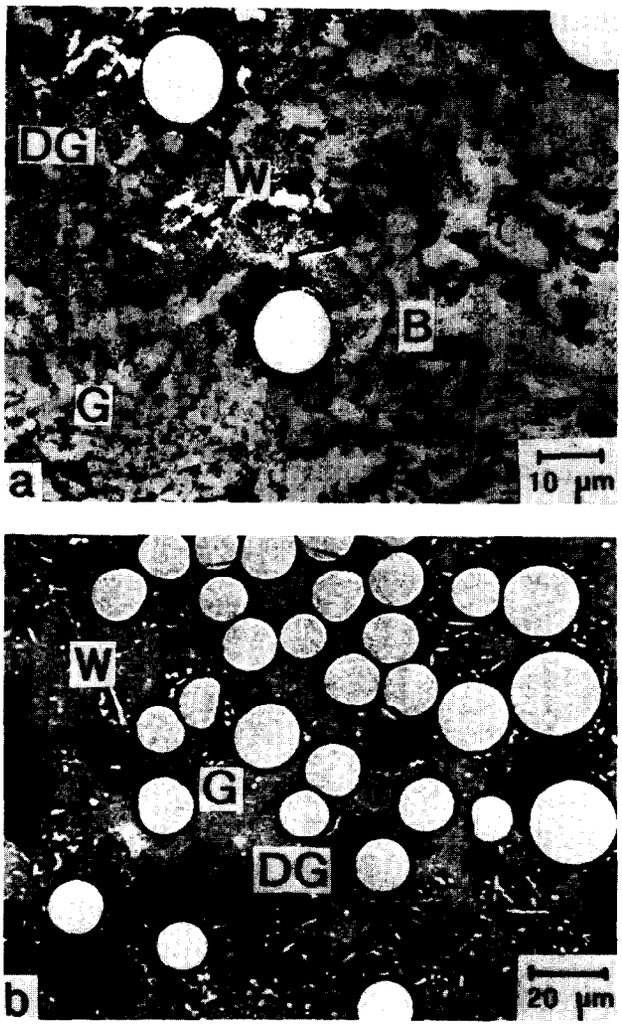

Fig. 9. Scanning electron micrographs of the MLAS matrices of the 1D (a) and 2D (b) composites (W = white: mullite, G = grey: cordierite, DG = dark grey: spodumene, B = black: carbon).

Results

Because of their very fine microstructure the composites have been investigated by scanning and transmission electron microscopies with microanalysis. The identification of the different present phases was confirmed regularly by X-ray analysis, EDS spectra and from the diffraction patterns.

SiC_f–MLAS

Although the 1D and 2D SiC_f–MLAS composites were elaborated in similar conditions, the as-received materials themselves differ, by several points. From observations and images of the MLAS matrix by scanning electron microscopy, it appears for the 2D materials white (W), grey (G) and dark grey (DG) areas, while for the 1D materials in addition there are black zones (B), (Figs 9(a) and (b)). All these phases seem to be not uniformally distributed inside the matrix.

The white phase was analyzed as mullite ($Al_6Si_2O_{13}$) as it coincides to crystals, generally elongated (Fig.10) and richer in aluminum than in silicon, with the correct ratio. The mullite crystals appear square section like. They are spread throughout the matrix with no particular orientation. The mullite needle shape is not so clearly observed in the 1D composite compared to the 2D ones. Moreover, the amount of mullite crystals is greater in the 2D than in the 1D materials. TEM

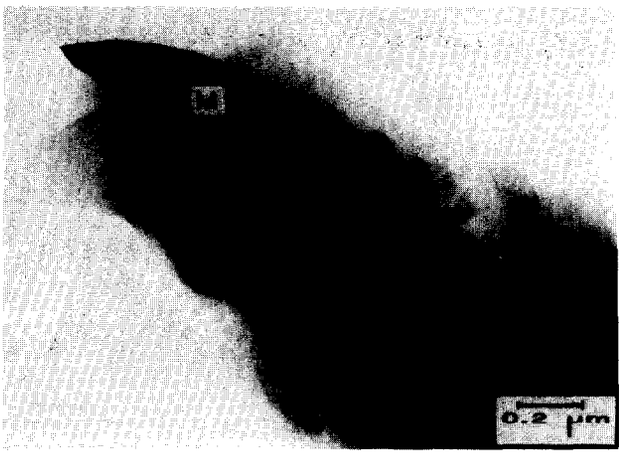

Fig. 10. TEM micrograph showing a mullite (M) needle in Bragg's conditions.

observations realised on the 1D composites show that these needles are sometimes surrounded by large crystals identified as β spodumene.

The dark-grey phase corresponds to the main phase only in the 1D materials: these areas are richer in silicon than in aluminum. Inside this phase the presence of magnesium is also detected. The presence of Mg is always detected whatever the phase is analyzed: mullite was even containing very few percent of Mg. By considering the Si/Al ratio and the diffraction patterns, the dark-grey phase was identified as β spodumene ($LiAlSi_2O_6$) or to a solid solution of β spodumene whose lithium cannot be detected, and where the magnesium ratio is not always the same in the whole specimen. The 1D composite investigated in TEM confirms that the main phase is β spodumene with quite large grains (Fig. 11). In the 2D materials, β spodumene zones appear only as inclusions dispersed in the grey phase.

These inclusions, recognised as β spodumene, have also been observed in 2D as-received SiC_f–MLAS composites, having a size greater than 100 nm.[33] The grey phase corresponding to the main phase in the 2D materials is the one richest in magnesium. Although the amount of magnesium is always lower than the theoretical value predicted from β cordierite formula ($Mg_2Al_4Si_5O_{18}$) this phase has been recognised as β cordierite or as a solid solution of β cordierite. These results of cordierite in the 2D material need further complementary investigations. In the 1D material β cordierite crystals have never been observed alone but always near to β spodumene crystals (Fig. 12).

Finally in the 1D materials one also observes black zones corresponding to areas with a very high concentration of carbon. This probably comes from the decomposition of organic compounds used during the fabrication of these composites as no carbon is used to coat the silicon fibers during the process route. Observations in TEM agree with this presence of carbon. Figure 13 shows carbon patches inside a β spodumene grain.

With regard to the fiber/matrix interface one observes several phases and turbostratic carbon layers. Close to the fiber side, EDS analysis gives

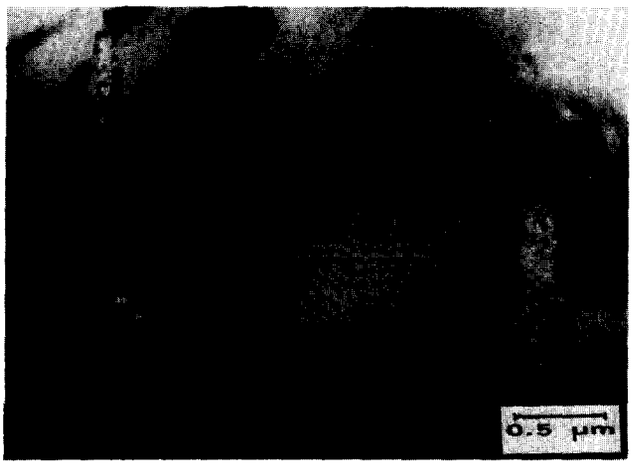

Fig. 11. Large grain of β spodumene observed in the 1D SiC_f–MLAS composite.

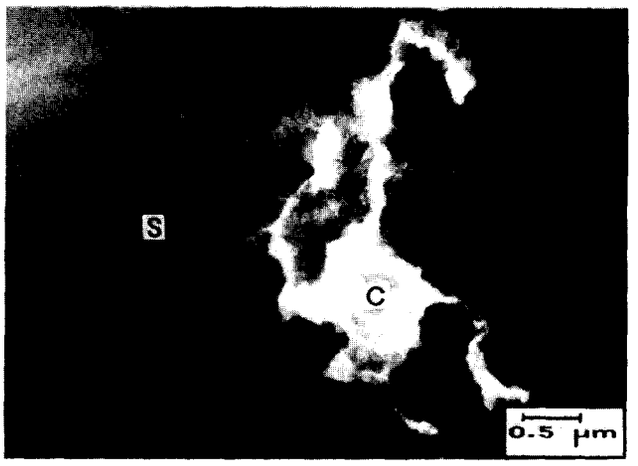

Fig. 13. Presence in the 1D composite of large carbon patches (C) inside spodumene grain (S).

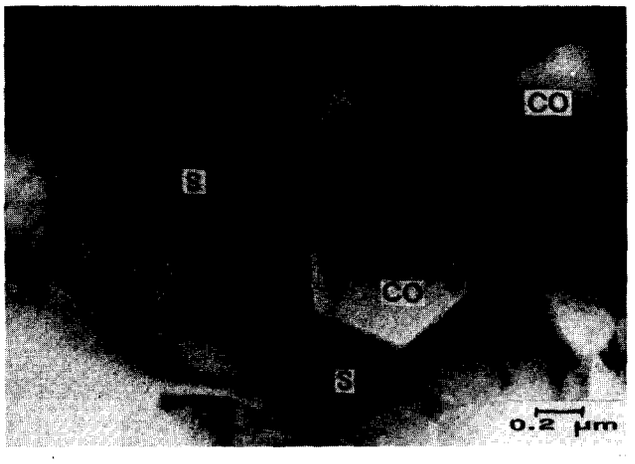

Fig. 12. Close mixture of β cordierite (CO) and β spodumene (S) grains in the 1D composite.

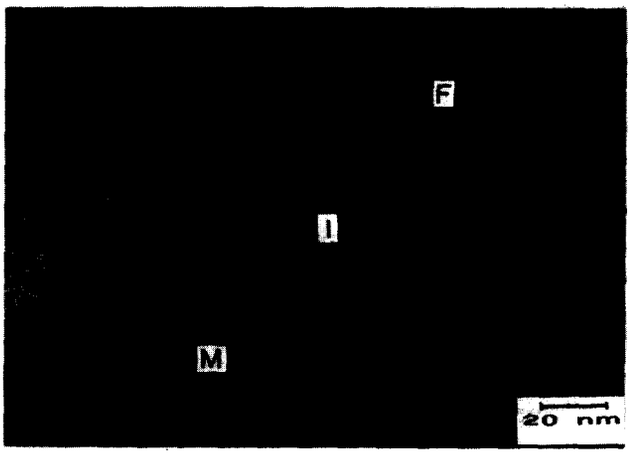

Fig. 14. Interface (I) between SiC fiber (F) and MLAS matrix (M) exhibiting mainly turbostratic carbon.

more silicon and oxygen and at the matrix side there is also a quite extended area along which the matrix appears to have reacted,[34] (Fig. 14). In these materials the interphase areas have a thickness which can vary from 10 to 100 nm.

SiC_f–YMAS

Figures 15(a) and (b) present the scanning electron micrographs of each composite. The phase containing yttrium appears in white. Large grains of that phase are present in Composite A. After microanalysis they have been identified as an yttrium silicate compound.[35] Due to the probe size (2 μm^3) it has not been possible to identify the small white grains as yttrium silicate. The black areas (Fig. 15(b)) show a phase rich in aluminum, magnesium and silicon elements, without the presence of yttrium. Composite B presents a more homogeneous microstructure without the presence of large grains. Globally the microstructure of these two types of composite is too fine to be analyzed at that scale because of the classical probe size used. Observations of Composite A reveals the existence of two main phases appearing in black and white. The dark crystals are distributed in a complex network and are elongated with a dendritic shape. Most of the yttrium phase is located in these zones (Fig. 16). The yttrium silicate has been identified as the high temperature form. The white areas generally correspond to more homogeneous zones. They are formed with cordierite crystals (the high cordierite) with a hexagonal symmetry (Fig 16).

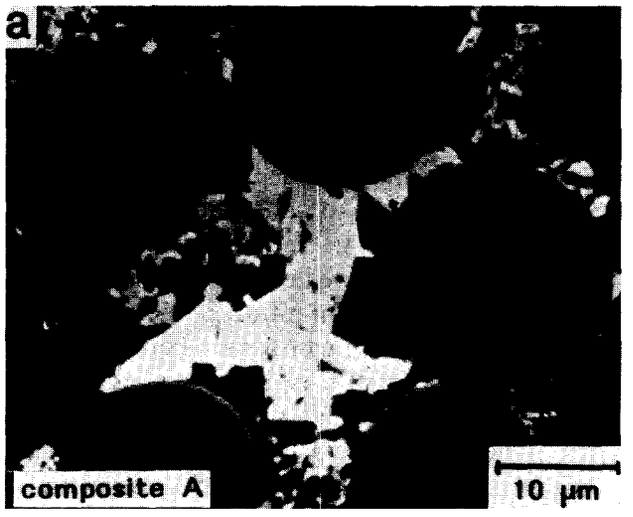

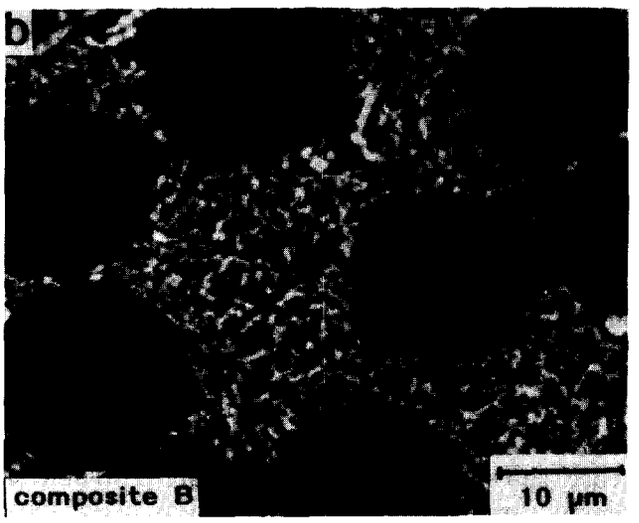

Fig. 15. SEM micrographs of the SiC_f–YMAS composite prepared by the sol–gel route (a) and by the glassy route (b).

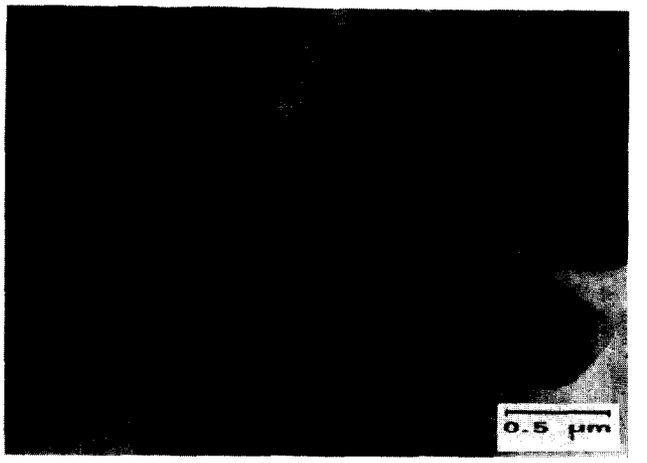

Fig. 16. Matrix formed by a network of yttrium silicate crystals with dendritic shape (dark) inside cordierite phase (clear), in Composite A.

For Composite A, some areas with a totally different microstructure also appear. An example is shown in Fig. 17. In that case, elongated and square shaped crystals are present in a phase which corresponds to a mixture of cordierite and yttrium silicate. These crystals were identified as mullite ($Al_6Si_2O_{13}$). Moreover some spinel crystals ($MgAl_2O_4$) are often observed within the cordierite or in the grain boundaries (Fig. 18)

Composite B exhibits the main microstructural features as Composite A. However, mullite crystals are rarely observed and the matrix appears finer and more homogeneous. In addition it has been observed that the cordierite crystals contain

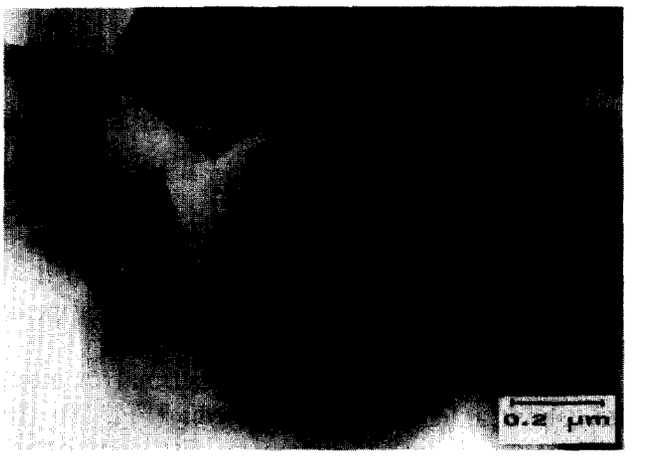

Fig. 17. Example of mullite crystal inside a mixture of yttrium silicate and cordierite in Composite A.

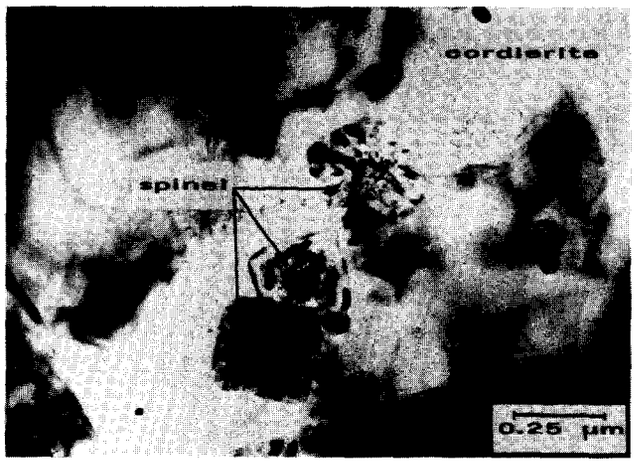

Fig. 18. Spinel crystals inside cordierite grain in Composite A.

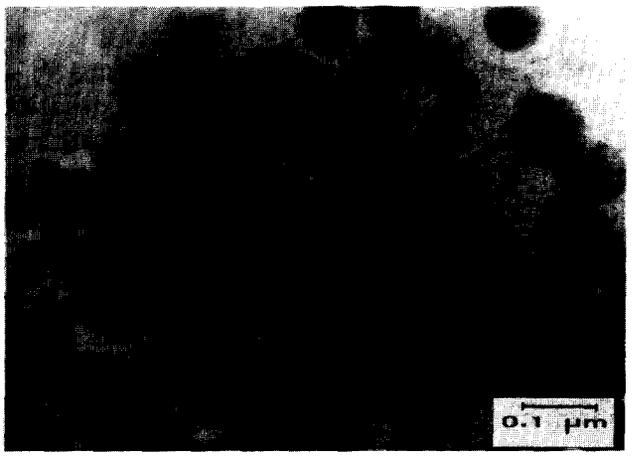

Fig. 19. Zirconia crystals inside cordierite phase in Composite B.

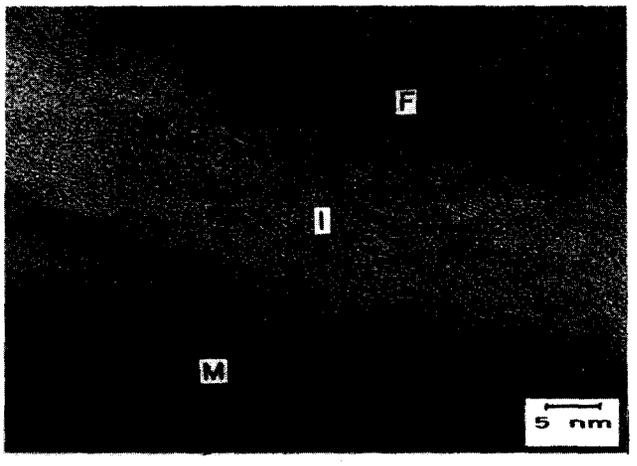

Fig. 20. HREM micrograph of the fiber/matrix interface, in Composite B.

some small inclusions (~20–100 nm) identified as zirconia (Fig. 19). At this scale, the matrix appears totally crystallized.

HREM observations at the fiber/matrix interface show a light contrasted layer (Fig. 20). Its thickness is about 20–30 nm in both composites. The nanostructure of the interface is similar to that one observed by Monthioux[36] in another type of glass ceramic composite (SiC_f–MLAS), with a layer of turbostratic carbon The sharp interface observed in the matrix side of the carbon layer and the diffuse interface observed on the Nicalon SiC fiber. support the concept of a carbon layer growing in the fiber.

Discussion

SiC_f–MLAS

The glass composite we had for the MLAS matrix — $0{\cdot}5MgO–0{\cdot}5Li_2O–1Al_2O_3–4SiO_2$ — is supposed to give as the first major phase, β eucryptite solid solution. As an immiscibility dome between SiO_2 and $Li_2O–Al_2O_3$ exists, one can have either a glass with the expected composition or a glass which can be richer or poorer in SiO_2 than expected. This leads to a β eucryptite solid solution in the LAS system whose composition can be quite far from the theoretical formula $Li_2O–Al_2O_3–2SiO_2$.[37]

The β eucryptite phase is subjected to microcracking and therefore has poor mechanical properties.[16] It is why one seeks to invert β eucryptite into β spodumene in this system. This transformation is possible whenever a glass composition has at least $3{\cdot}5SiO_2$ for $1MgO$ and $1Li_2O$[38] By heating the previous solid solution at 1050°C the transformation takes place and a β spodumene solid solution appears. This phase is suitable for thermomechanical applications generally because no microcracking appears. Moreover, it has recently been shown that this phase can be corroded easily by boiling sulfuric acid or by molten sodium nitrate.[39]

The precursor phase can have a composition in quite a large range, so it is not surprising that for the β spodumene a solid solution with different ratios of elements can crystallize.

At higher temperatures the MAS system (Fig. 4) considers the formation of β cordierite which also has no stable composition, particularly in magnesium. But substitution between Li^+ and Mg^{2+} are quite easy as they have a close ionic radii (Li^+:0·68 Å; Mg^{2+}:0·78 Å).

The presence of mullite crystals is evident in both the LAS and MAS systems (Figs 1 and 4) as they contain its existence domain.

The noticeable differences between the 1D and 2D materials in terms of majority phases is perhaps shown in the pseudo binary diagram cordierite–spodumene (Fig. 3).[8] To our knowledge this is the only one which makes a junction between the LAS and the MAS systems. Its existence shows that liquid phases are available at temperatures in the ternary diagrams taken separately. According to this diagram and depending upon the predominant phase in a cordierite–

spodumene mixture two different situations can arise. On one hand if we have more cordierite than spodu- mene a heat treatment will lead to even more cordierite and then to mullite. On the other hand a mixture richer in spodumene will give even more spodumene and less cordierite.

The association of cordierite and mullite was also predicted in Refs 13 and 14. It was noticed that in the MAS diagram the cordierite is able to melt incongruently by giving mullite at a temperature between 1355 and 1465°C.

In conclusion, the 1D SiC_f–MLAS matrix seems to belong to a system which has at the beginning more β spodumene than β cordierite, whilst for the 2D matrix it is the opposite. The materials evolution during creep tests confirm this assumption, as the 1D was evolving towards the β cordierite disparition to the benefit of β spodumene.[10] Concerning the 2D materials, no evolution between spodumene and cordierite has been reported as yet, but great enhancement of mullite crystals has been evident.

SiC_f–YMAS

Whatever the YMAS composites (A or B) one considers that the matrix contains two major and two minor phases, that is to say cordierite and yttrium silicate for the major and spinel and mullite for the minor. Besides this, zircone inclusions have been found in composite B. This can be easily explained by the oxide used in order to enhance the crystallization in the glassy route.

Microstructural observations and analyses on these materials have shown that yttrium silicate is the only compound which contains yttrium. This is in good agreement with previous investigations.[30,40] So it can be supposed that all the Y_2O_3 reacts with SiO_2 to form the $Y_2Si_2O_7$ phase.

Diffraction patterns allows us to identify the β form of that oxide. Because of the temperature of fabrication, it is in good agreement with the literature despite the fact that many temperatures are given for the same allotropic transformation according to different authors (cf. Table 2).

As yttrine is only in the $Y_2Si_2O_7$ silicate form, one can consider that alumina and magnesia react together to give binary or ternary compounds by reaction with silica as well. This leads us to consider the MAS system.

Moreover if one considers the amount of remaining silica, alumina and magnesia, it corresponds to a composition close to the sapphirine, which is present in the MAS ternary diagram. Unfortunately this phase has not been detected, but its existence domain is very small (Fig. 4). On that diagram one also notes that this phase is surrounded by three large domains corresponding to the three other phases identified in our composites, i.e. cordierite, mullite and spinel.

The cordierite is the second major phase with the yttrium silicate. It has been previously shown[13,14] that its formation by sintering begins at 1200°C. From the MAS diagram (Fig. 4) it appears as the phase existing at the lowest temperature domain. That is the reason why that phase appears as the most important at that fabrication temperature.

Very few mullite crystals appear in the YMAS matrix as silica reacts first to form cordierite rather than mullite because of its lower temperature of sintering (1200°C): that is in good agreement with the process temperature. As for the excess in magnesia, it reacts with alumina to form spinel above 1000°C.

Conclusion

The development of glass ceramic matrices is important in the field of ceramic matrix composites (CMCs) due to their very low thermal expansion coefficient and their good mechanical strength. So it requires a good knowledge of the corresponding pseudo–binary, ternary and quaternary diagrams. From their accurate analysis one can note many important difficulties: (i) different silicate phases can appear in very close domains; (ii) many allotropic transformations exist; (iii) different atom substitutions can arise and (iv) several crystallographic parameters of different silicate phases have the same value. These different points emphasize the complexity of knowing with accuracy which phases are present in the materials. Anyway, during long term applications, these silicate phases can evolve.

The management (control) of the stability of the glass ceramic matrices in these multicomponent systems is an essential step to consider applications for long durations, such as for motors, hypersonic structures, etc.... Moreover, for glass ceramic systems with aluminum or lithium reinforced by silicon carbide fibers, such as LAS, MAS, YAS, MLAS or YMAS systems, the diffusion of aluminum or lithium in the SiC fibers is an important factor to consider: it can act on the crystalline phases of the matrix due to change in composition and can make the fibers even more brittle. Moreover a matrix with lithium or lithium components can evaporate during the process.[41]

These different points have been illustrated by investigations in scanning and transmission electron microscopies with microanalysis, of the MLAS ($MgO–Li_2O–Al_2O_3–SiO_2$) and YMAS ($Y_2O_3–MgO–Al_2O_3–SiO_2$) systems.

It appears that the matrices in the 1D and 2D SiC_f–MLAS composites are slightly different, although the composition of the started gel and the process were the same. This simple fact shows the difficulty in obtaining any point reproductible matrices with exactly the same phases and distributions.

This is due to the multitude of possibilities deduced from the thermodynamic diagrams. In fact the detectable phases in the two composites are identical but their size distribution is not. The 1D matrix shows the following phase distribution: β spodumene > β cordierite >> ϵ mullite, while in the 2D it is β cordierite >> β spodumene > mullite. Consequently when the SiC_f–MLAS composites are submitted to creep test, the matrix which is not totally crystallized, will be subjected to chemical and morphological evolution. As the as-received matrices are not exactly equivalent, different ways of phase evolution will have to be considered. But depending on which scale we are working, these phenomena will be considered as crucial or as minor: for example, if one has to compare the damage due to a crack running from one ply to another with regard to a phase transformation.

The main phases in YMAS matrices were β $Y_2Si_2O_7$ and β cordierite, the secondary ones being mullite and spinel. It is maintained by a very complex network acting like a spider's web where minor and major phases are sometimes overlapping. One other advantage of this system is that no substitution can occur between magnesium and yttrium.

In the two YMAS and MLAS matrices one expects a more stable YMAS type matrix because this one is totally crystallized.

Acknowledgements

This work has been performed: (i) in the frame of the Groupement Scientifique GS 4C 'Comportements thermomécaniques des composites céramique–céramique à fibre' supported by CNES, CNRS, DRET, MRE and Aerospatiale, SEP and SNECMA companies, and (ii) under DRET contract no. 92/1221 A.

The authors want to warmly thank their colleagues Dr T. Chartier and Pr. B. T. Frit (URA CNRS n°320, Limoges, France), Mrs M. H. Ritti, Mr T. Grenier and Dr M. Parlier (ONERA, Châtillon sous Bagneux, France), Dr G. Larnac (Aérospatiale Company, Etablissement de Bordeaux, France) and Dr R. Pompe (Swedish Institute for Silicate Research, Göteborg, Sweden), for fruitful discussions.

References

1. Long, M. & Moore, R. E., Development of glass ceramic matrix composites for aircraft applications, *Sil. Ind.*, **7–8** (1990) 223–9.
2. Partridge, G., Elyard, C. A., Budd, M. I., Glass ceramics in substrate applications. In *Glasses and Glass-Ceramics*, ed. M. H. Lewis, Chapman and Hall, 1988 pp. 226–71.
3. Scheidler, H., Rodek, E., Li_2O–Al_2O_3–SiO_2 glass ceramics *Amer. Ceram. Bull.*, **68**(11) (1989) 1926–30.
4. Roy, R., & Osborn, E. F., The system lithium metasilicate spodumene silica, *J. Amer. Chem. Soc.*, **71** (1949) 2086–95.
5. Roy R., Roy, D. M. & Osborn, E. F., Compositional and stability relationships among the lithium aluminosilicates: eucryptite, spodumene, and petalite, *J. Amer. Ceram. Soc.*, **33**(5) (1950) 152–9.
6. Hatch, R. A., Phase equilibrium in the system: Li_2O–Al_2O_3–SiO_2, *Amer. Mineral.*, **28** (1943) 471–96.
7. Strnad, Z., Glass-ceramic materials, liquid phase separation, nucleation and crystallization. In *Glass Science and Technology 8*, Elsevier, 1986 pp. 76–89.
8. Karkhanavala, M. D. & Hummel, F. A., Reactions in the system Li_2O–MgO–Al_2O_3–SiO_2: I The cordierite–spodumene join, *J. Amer. Ceram. Soc.*, **36**(12) (1953) 393–7.
9. Gouby, I., Les cordiérites dopées aux alcalins. Influences du traitement thermique sur la structure cristalline et sur quelques propriétés physiques, Thèse de l'Université de Limoges, Feb. 1994.
10. Kervadec, D., Comportement en fluage sous flexion et microstructure d'un SiC_f–MLAS 1D, Thèse de Doctorat de l'Université de Caen, Dec. 1992.
11. Winkler, H. G. F., Synthese und Kristallstruktur des Eukryptits, $LiAlSiO_4$, *Acta. Cryst.* **1**(1) (1948) 27–34.
12. Prokopowicz, T. I., & Hummel, F. A., Reactions in the system Li_2O–MgO–Al_2O_3–SiO_2: II Phase equilibria in the high-silica region, *J. Amer. Ceram. Soc.*, **39**(8) (1956) 266–78.
13. Osborn, E. F. & Muan, A., (1961) cited by Jouenne, C. A., (1984).
14. Jouenne, C. A., *Traité de Céramiques et Matériaux Minéraux*, Editions Septima, 1984, pp. 185–7.
15. Beall, G. H., Karstetter, B. R. & Rittler, H. L., Crystallization and chemical strengthening of stuffed β-quartz glass ceramics, *J. Amer. Ceram. Soc.*, **50**(4) (1967) 181–90.
16. Larnac, G., Elaboration d'une matrice pour composites céramique–céramique par la voie sol–gel, Thèse de l'Université des Sciences et Techniques du Languedoc, Université de Montpellier II, April 1990.
17. Barry, T. I., Cox, J. M. & Morrell, R., Cordierite glass-ceramics-effect of TiO_2 and ZrO_2 content on phase sequence during heat treatment, *J. Mat. Sci.*, **13**(3) (1978) 594–610.
18. Coon, D. N., Simultaneous sintering and crystallization of a M_9O–Li_2O–Al_2O_3–SiO_2 glass powder, *J. Mat. Sci. Let.*, **7**(11) (1983) 1181–3.
19. Coon, D. N. & Neilson, R. M., Effect of M_9O additions on the glass transition temperature of LiO_2–Al_2O_3–SiO_2 glasses, *J. Mat. Sci. Let.*, **7**(1) (1988) 33–5.
20. Ray, S. & Muchow, G. M., High-quartz solid solution phases from thermally crystallized glasses of compositions, *J. Amer. Ceram. Soc.*, **51**(12) (1968) 678–82.
21. Mazza, D. & Lucco-Borlera, M., Effect of the substitution of boron for aluminum in the β-eucryptite $LiAlSiO_4$ structure, *J. Eur. Ceram. Soc.*, **13**(1) (1994) 61–5.
22. O'Meara, C. O., Dunlop, G. L. & Pompe, R., Phase relationships in the system SiO_2–Y_2O_3–Al_2O_3, In *6th CIMTEC*, ed. P. Vincenzini, Elsevier, 1987. pp. 265–70.
23. Hyatt, M. J. & Day, D. E., Glass properties in the yttria–alumina–silica system, *J. Amer. Ceram. Soc.*, **70**(10) (1987) C283–7.
24. Bondar, A. & Galakhov, F. Ya, Phase equilibria in the system Y_2O_3–Al_2O_3–SiO_2, *Izv. Akad. Nauk. SSSR, Ser. Khim*, **7** (1964) 1325–6.

25. Ito, J. & Johnson, H., Synthesis and study of yttrialite, *Amer. Mineral.*, **53** (Nov.–Dec.) (1968) 1940–52.
26. Felsche, J., Crystal data on the polymorphism of disilicate $Y_2Si_2O_7$, *Die Naturwissenschaften*, **57**(3) (1970) 127–8.
27. Liddell, K. & Thompson, D. P., X-ray diffraction data for yttrium silicates, *Brit Ceram. Trans. J.*, **85** (1986) 17–22.
28. Lee, W. E. & Hilmas, G. E., Microstructural changes in β–Si_3N_4 grains upon crystallizing the grain-boundary glass, *J. Amer. Ceram. Soc.*, **72**(10) (1989) 1931–7.
29. Arita, I. H., Wilkinson, D. S. & Purdy, G. R., Crystallization of yttria–aluminina–silica glasses, *J. Amer. Ceram. Soc.*, **75**(12) (1992) 3315–20.
30. Séraudie, C., Elaboration et propriétés thermomécaniques de composites à fibres de carbure de silicium et matrices vitrocéramiques, Thése de Doctorat de l'Université de Limoges, July 1990.
31. Grenier, T., Parent, P. & Parlier, M., Elaboration de composites SiC_f–MASY à l'échelle quart de grand, Technical Report ONERA-DRET 2–3762 MY, Aug. 1994.
32. Larnac, G., Pérès, P. & Donzac., J. M., Elaboration et caractérisation du composite à matrice vitrocéramique SiC–MASL., *Rev. Comp. Mat. Avancés*, **3 HS**, (1993) 27–41.
33. Backhaus–Ricoult, M., Mozdzierz, N., Imhoff, D., Eveno, P., Deschamps, J., Pelissier, B., Miloche, M. & Bahezre, C., Final Report on GS 4C, Comportments thermomécaniques des composites céramique–céramique à fibres, Jan. (1994).
34. Ruterana, P., Kervadec, D., Maupas, H. & Chermant, J. L., Microstructure and evolution of a *MLAS* matrix composite. In *Microscopy of Composite Materials II*, Oxford, UK, 11–13 April 1994. To appear in *J. Microscopy*, **177**(3) (1995) 272–8.
35. Vicens, J., Doreau, F. & Chermant, J. L., Microstructure of experimental SiC_f–YMAS type CMC materials, In *Microscopy of Composite Materials II*, Oxford, UK, 11–13, April 1994. *J. Microscopy* (1995), **177**(3) (1995) 242–50.
36. Monthioux, R., Nano et microstructure de composites SiC/MASL, *Rev. Comp. Mat. Avancés*, **3 HS**, (1993) 69–90.
37. Gillery, F. H & Buch, E. A., Thermal contraction of β-eucryptite (Li_2O–Al_2O_3–$2SiO_2$) by X-ray and dilatometry methods, *J. Amer. Ceram. Soc.*, **42**(4) (1949) 175–7.
38. Eppler, R. A., Glass formation and recrystallization in the lithium metasilicate region of the system Li_2O–Al_2O_3–SiO_2, *J. Amer. Ceram. Soc.*, **46**(4) (1963) 97–101.
39. Colomban, P., Ion exchange, fiber/silicates matrix reactions and hot corrosion in glass ceramic and ceramic matrix composites, 3rd Int. Conference on Ceramic–Ceramic Composites CCC–III. Mons, Belg., Oct. 18–20 1994 *Sil. Ind.* (1995), in press.
40. Nussbaum, H. & Montardi, Y., Elaboration et caractérisation de céramiques. Composites à matrice verre, Report Rhône–Poulenc, n°. 86/016, BC 26 (1988)
41. Chartier, T., Private communication (1994).